Article

Cation-Modulated Electron-Transfer Channel: H-Atom Transfer vs Proton-Coupled Electron Transfer with a Variable Electron-Transfer Channel in Acylamide Units

Xiaohua Chen, and Yuxiang Bu

J. Am. Chem. Soc., **2007**, 129 (31), 9713-9720• DOI: 10.1021/ja071194m • Publication Date (Web): 18 July 2007

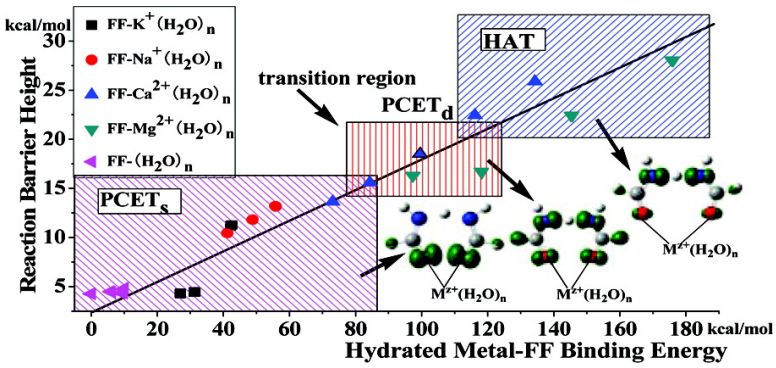

More About This Article

Additional resources and features associated with this article are available within the HTML version:

- Supporting Information
- Links to the 3 articles that cite this article, as of the time of this article download
- Access to high resolution figures
- Links to articles and content related to this article
- Copyright permission to reproduce figures and/or text from this article

View the Full Text HTML

J|A|C|S
ARTICLES
Published on Web 07/18/2007

Cation-Modulated Electron-Transfer Channel: H-Atom Transfer vs Proton-Coupled Electron Transfer with a Variable Electron-Transfer Channel in Acylamide Units

Xiaohua Chen and Yuxiang Bu*

Contribution from the Institute of Theoretical Chemistry, Shandong University, Jinan, 250100, People's Republic of China

Received February 19, 2007; E-mail: byx@sdu.edu.cn

Abstract: The mechanism of proton transfer (PT)/electron transfer (ET) in acylamide units was explored theoretically using density functional theory in a representative model (a cyclic coupling mode between formamide and the N-dehydrogenated formamidic radical, **FF**). In **FF**, PT/ET normally occurs via a seven-center cyclic proton-coupled electron transfer (PCET) mechanism with a N→N PT and an O→O ET. However, when different hydrated metal ions are bound to the two oxygen sites of **FF**, the PT/ET mechanism may significantly change. In addition to their inhibition of PT/ET rate, the hydrated metal ions can effectively regulate the **FF** PT/ET cooperative mechanism to produce a single pathway hydrogen atom transfer (HAT) or a flexible proton coupled electron transfer (PCET) mechanism by changing the ET channel. The regulation essentially originates from the change in the O···O bond strength in the transition state, subject to the binding ability of the hydrated metal ions. In general, the high valent metal ions and those with large binding energies can promote HAT, and the low valent metal ions and those with small binding energies favor PCET. Hydration may reduce the Lewis acidity of cations, and thus favor PCET. Good correlations among the binding energies, barrier heights, spin density distributions, O···O contacts, and hydrated metal ion properties have been found, which can be used to interpret the transition in the PT/ET mechanism. These findings regarding the modulation of the PT/ET pathway via hydrated metal ions may provide useful information for a greater understanding of PT/ET cooperative mechanisms, and a possible method for switching conductance in nanoelectronic devices.

Introduction

The acylamide unit is found in many biological species, such as peptide bonds, asparagine, glutamine, guanine, thymine/uracil, and flavin, etc.[1−4] Its radicals in some chemical or biological surroundings have emerged as prominent redox-active cofactors and charge transfer intermediates in enzyme reactions or DNA/protein damage. As verified in DNA duplexes, oxidative lesions of guanine may cause proton-coupled electron transfer (PCET), which provides a mechanism for charge transport.[5] Nature employs the acylamide unit mainly to fulfill two criteria: (1) formation of an H-bond network for protein helices and DNA base pairs and (2) possible participation in enzyme reactions. Clearly, such a special unit has provided the possibility of binding bioactive metal ions at its carbonyl site[6] and releasing its proton in some abnormal physiological conditions, such as oxidative lesions. Our recent studies have highlighted some special properties of the protons associated with the acylamide unit in oxidization or metal cation coupling cases.[7]

Metal ions are a class of important components in vivo and play a vital role in regulating the biological functionality of active centers. In particular, recent studies reveal that metal ions or their complexes can efficiently influence the pathway and rate of electron transfer (ET).[8] For example, Sc^{3+} ion binding at the electron acceptor can change the ET mechanism in CoTPP−O_2 from a one-step hydride transfer (H^-) to ET followed by a proton transfer (PT) and an electron transfer

(1) Biological residues containing acylamide units include peptide bonds, asparagine, glutamine, guanine, thymine/uracil, and flavin. The acylamide unit has two tautomers: *cis*-H and *trans*-H, as in peptide bonds, asparagine and glutamine, etc., but some only have a *cis*-H conformer, as in guanine, thymine/uracil, and flavin. In many cases, the *cis*-H tautomers are located near protein active sites and may play an important role in the functioning of enzymes (refs 2−4).

(2) Ramachandran, G. N.; Sasisekharan, V. *Adv. Prot. Chem.* **1968**, *23*, 283−437.
(3) (a) Weiss, M. S.; Jabs, A.; Hilgenfeld, R. *Nat. Struct. Biol.* **1998**, *5*, 676−676. (b) Jabs, A.; Weiss, M. S.; Hilgenfeld, R. *J. Mol. Biol.* **1999**, *286*, 291−304.
(4) (a) Herzberg, O.; Moult, J. *Proteins: Struct. Funct. Genet.* **1991**, *11*, 223−229. (b) Stoddard, B. L.; Pietrokovski, S. *Nat. Struct. Biol.* **1998**, *5*, 3−5.
(5) (a) Weatherly, S. C.; Yang, I. V.; Thorp, H. H. *J. Am. Chem. Soc.* **2001**, *123*, 1236−1237. (b) Shafirovich, V.; Dourandin, A.; Geacintov, N. E. *J. Phys. Chem. B* **2001**, *105*, 8431−8435. (c) Milligan, J. R.; Aguilera, J. A.; Hoang, O.; Ly, A.; Tran, N. Q.; Ward, J. F. *J. Am. Chem. Soc.* **2004**, *126*, 1682−1687.
(6) Alberts, B.; Bray, D.; Lewis, J.; Raff, M.; Roberts, K.; Watson, J. D. *Molecular Biology of the Cell*; Garland Science: New York, 2002. (a) Cerda, B. A.; Hoyau, S.; Ohanessian, G.; Wesdemiotis, C. *J. Am. Chem. Soc.* **1998**, *120*, 2437−2448. (b) Kohtani, M.; Kinnear, B. S.; Jarrold, M. F. *J. Am. Chem. Soc.* **2000**, *122*, 12377−12378. (c) Wong, C. H. S.; Ma, N. L.; Tsang, C. W. *Chem. Eur. J.* **2002**, *8*, 4909−4918.
(7) (a) Li, P.; Bu, Y. *J. Phys. Chem. A* **2004**, *108*, 10288−10295. (b) Sun, L.; Bu, Y. *J. Phys. Chem. B* **2005**, *109*, 593−600. (c) Li, H.; Bu, Y.; Yan, S.; Li, P.; Cukier, R. I. *J. Phys. Chem. B* **2006**, *110*, 11005−11013.
(8) (a) Fukuzumi, S.; Patz, M.; Suenobu, T.; Kuwahara, Y.; Itoh, S. *J. Am. Chem. Soc.* **1999**, *121*, 1605−1606. (b) Fukuzumi, S.; Ohkubo, K. *Chem. Eur. J.* **2000**, *6*, 4532−4535. (c) Ohkubo, K.; Suenobu, T.; Imahori, H.; Orita, A.; Otera. J.; Fukuzumi, S. *Chem. Lett.* **2001**, *30*, 978−979.

(e + H^+ +e).[8a,b] Certainly, changing Sc^{3+} to other metal ions may yield different effects on the cooperativity of these (2e + H^+) migrations.[8c] In addition, a hydrated Na^+ ion, more readily than hydrated K^+ ion, can penetrate into some active zones, to modulate electron hole migration in DNA.[9] On the other hand, incorporation of metal ions into electron donor-linked electron acceptor intermolecular or intramolecular assemblies allows control of the coupling modes and magnitudes between the donor and acceptor sites, which govern the channel, rate, and efficiency of ET.[10]

Clearly, the concept of catalytic modulation of ET reactions, especially the complicated PCET reactions, provides a new perspective on ET chemistry, expanding the scope of ET systems, which would otherwise be impossible to study. It has been demonstrated that binding of a metal ion with a substrate radical plays an important role in the catalytic control of ET reactions.[8] The catalytic effects (promoting or inhibiting) of metal ions on ET reactions are related not only to the binding site but also to the Lewis acidity of the metal ions.

Recently, an interesting theoretical study was reported on the iminoxyl/oxime self-exchange reaction, which occurs by a five-center, cyclic PCET mechanism with the proton being transferred between electron pairs on the oxygens, and the electron migrating between in-plane orbitals on the two nitrogens.[11] Motivated by this special PCET mechanism, and on the basis of investigations of peptide bond protons, we examined the radical exchange between an acylamide unit and its oxidative lesion-generated radical. Interestingly, similar cyclic structures for both reactant and the PT/ET transition state were found. Furthermore, stimulating our continuing exploration is the possibility of a PT/ET pathway in which a proton and an electron may also cooperatively transfer from one molecular fragment to another via two different channels. Seemingly, these two mechanisms should be similar. However, careful inspection reveals that, in contrast to the iminoxyl/oxime radical exchange reaction, the formation of such a cyclic structure requires an anti-electronegativity-rule ET from the more electronegative oxygen atom to the less electronegative nitrogen atom that is thermodynamically nonspontaneous (forbidden) for the radical fragment. Undoubtedly, such a radical exchange process is associated with the structural characteristics of acylamide units and the PT/ET mechanism and certainly deserves a more detailed investigation. Further, it has yet to be determined whether PT/ET in such a cyclic acylamide complex is controllable or not. Additionally, the ET process usually accompanies PT simultaneously, which may then be mainly classified as a hydrogen atom transfer (HAT),[12−15] or as a more complicated PCET[11,15,16] process, with the latter further subdivided into several distinct types according to different reaction characteristics.[11,15] Clearly, knowledge about the PT/ET pathway and the cation-modulation of such exchange reactions is needed for investigation of this special unit in untangling relevant PCET mechanisms. Detailed mechanistic studies may also provide new insights into fundamental aspects of inorganic chemistry, molecular biology, and cellular physiology, especially the enzymatic processes with metal ion participations.

Scheme 1. Schematic Representation of the Considered Structures

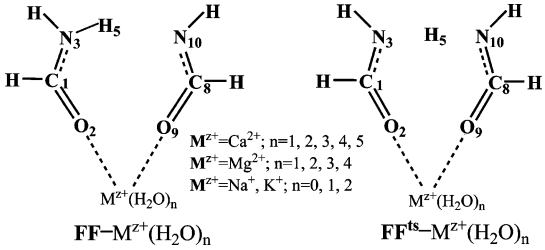

In this work, we show that hydrated metal ions can regulate the PT/ET cooperative mechanism between HAT and PCET with variable ET channels associated with the acylamide units.

General Considerations and Computational Details

In our work we employed formamide (**F**) to mimic the acylamide unit and probe the PT/ET radical exchange reaction with N-dehydrogenated formamidic radical (**Fr**), in a cyclic mode (**FF**, Figure S1), because of its extensive use as a model for acylamide units.[17−21] To understand the **FF** PT/ET reactivity in different environments and the modulating role of biologically significant metal ions, some of the extensively occurring bioactive metal ions, such as Na^+, K^+, Mg^{2+}, Ca^{2+}, etc.,[6] were considered to catalyze the PT/ET exchange reactions. A series of binding modes of the hydrated metal ions on two oxygen sites of **FF**, designated as **FF**-$M^{z+}(H_2O)_n$ (M^{z+} = Na^+, K^+, Mg^{2+}, Ca^{2+}; *n*, the water number in M^{z+} hydration shell), with the corresponding transition states **FF**^{ts}-$M^{z+}(H_2O)_n$ (Scheme 1), were located in the present work.

(9) (a) Barnett, R. N.; Cleveland, C. L.; Joy, A.; Landman, U.; Schuster, G. B. *Science* **2001**, *294*, 567−571. (b) Ponomarev, S. Y.; Thayer, K. M.; Beveridge, D. L. *Proc. Natl. Acad. Sci. U.S. A* **2004**, *101*, 14771−14775. (c) Varnai, P.; Zakrzewska, K. *Nucl. Acids Res.* **2004**, *32*, 4269−4280. (d) Savelyev, A.; Papoian, G. A. *J. Am. Chem. Soc.* **2006**, *128*, 14506−14518.

(10) Examples of metal ion modulated electron transfer reactions are: Fc-(M_1P)-(M_2P)-C_{60} ↔ Fc^+-(M_1P)-(M_2P)-C_{60}^-, where Fc = ferrocene; P^{2-} = porphyrin dianion derivative; M_1 and M_2 may be different metal ions or H^+. The electron exchange between the electron donor Fc and the acceptor C_{60} may be modulated by changing the metal ions. See also (a) Fukuzumi, S. *Org. Biomol. Chem.* **2003**, *1*, 609−620, and references therein. (b) Imahori, H.; Guldi, D. M.; Tamaki, K.; Yoshida, Y.; Luo, C.; Sakata, Y.; Fukuzumi, S. *J. Am. Chem. Soc.* **2001**, *123*, 6617−6628.

(11) DiLabio, G. A.; Ingold, K. U. *J. Am. Chem. Soc.* **2005**, *127*, 6693−6699.

(12) Isborn, C.; Hrovat, D. A.; Borden, W. T.; Mayer, J. M.; Carpenter, B. K. *J. Am. Chem. Soc.* **2005**, *127*, 5794−5795.

(13) (a) Stubbe, J.; van der Donk, W. A. *Chem. Rev.* **1998**, *98*, 705−762. (b) Easton, C. J.; Merrett, M. C. *J. Am. Chem. Soc.* **1996**, *118*, 3035−3036. (c) Zhang, J.; Grills, D. C.; Huang, K. W.; Fujita, E.; Bullock, R. M. *J. Am. Chem. Soc.* **2005**, *127*, 15684−15685.

(14) (a) Roth, J. P.; Yoder, J. C.; Won, T.-J.; Mayer, J. M. *Science* **2001**, *294*, 2524−2526. (b) Tanner, C.; Manca, C.; Leutwyler, S. *Science* **2003**, *302*, 1736−1739.

(15) (a) Mayer, J. M.; Hrovat, D. A.; Thomas, J. L.; Borden, W. T. *J. Am. Chem. Soc.* **2002**, *124*, 11142−11147. (b) Olivella, S.; Anglada, J. M.; Solé, A.; Bofill, J. M. *Chem. Eur. J.* **2004**, *10*, 3404−3410. (c) Anglada, J. M. *J. Am. Chem. Soc.* **2004**, *126*, 9809−9820. (d) Rhile, I. J.; Mayer, J. M. *J. Am. Chem. Soc.* **2004**, *126*, 12718−12719. (f) Terecek, F.; Syrstad, E. A. *J. Am. Chem. Soc.* **2003**, *125*, 3553−3369.

(16) (a) Mayer, J. M. *Annu. Rev. Phys. Chem.* **2004**, *55*, 363−390. (b) Cukier, R. I. *J. Phys. Chem.* **1995**, *99*, 16101−16115. (c) Cukier, R. I. *J. Phys. Chem.* **1996**, *100*, 15428−15443. (d) Trammell, S. A.; Wimbish, J. C.; Odobel, F.; Gallagher, L. A.; Narula, P. M.; Meyer, T. J. *J. Am. Chem. Soc.* **1998**, *120*, 13248−13249. (e) Cukier, R. I.; Nocera, D. *Annu. Rev. Phys. Chem.* **1998**, *49*, 337−369. (f) Cukier, R. I. *J. Phys. Chem. B* **2002**, *106*, 1746−1757. (g) Hammes-Schiffer, S. *Acc. Chem. Res.* **2001**, *34*, 273−281. (h) Hammes-Schiffer, S. *ChemPhysChem* **2002**, *3*, 33−42.

(17) (a) Adalsteinsson, H.; Maulitz, A. H.; Bruice, T. C. *J. Am. Chem. Soc.* **1996**, *118*, 7689−7693. (b) Angela, N. T.; Nancy, S. T. *J. Phys. Chem. A* **2000**, *104*, 2985−2993. (c) Cabaleito-Lago, E. M.; Rios, M. A. *J. Chem. Phys.* **1999**, *110*, 6782−6791.

(18) (a) Johansson, A.; Collman, P.; Rothenberg, S.; Mckelvey, J. *J. Am. Chem. Soc.* **1974**, *96*, 3794−3800. (b) Hinton, J. F.; Harpool, R. D. *J. Am. Chem. Soc.* **1977**, *99*, 349−353. (c) Pullman, A.; Berthod, H.; Giessner-Prettre, C.; Hinton, J. F.; Harpool, D. *J. Am. Chem. Soc.* **1978**, *100*, 3991−3994. (d) Novoa, J. J.; Whangbo, M. H. *J. Am. Chem. Soc.* **1991**, *113*, 9017−9026.

(19) Mehler, E. L. *J. Am. Chem. Soc.* **1980**, *102*, 4051−4056.

(20) Muller, A.; Losada, M.; Leutwyler, S. *J. Phys. Chem. A* **2004**, *108*, 157−165.

(21) (a) Watson, T. M.; Hirst, J. D. *J. Phys. Chem. A* **2002**, *106*, 7858−7867. (b) Ireta, J.; Neugebauer, J.; Scheffler, M. *J. Phys. Chem. A* **2004**, *108*, 5692−5698.

Since the substrate (**FF**) exhibits a bidentate character when binding to the metal ions, the maximum number (n) of water molecules as the additional ligands was considered for each metal ion to be its saturated coordination number minus 2. For the alkali metal ions (Na^+, K^+), it has been shown that they prefer to coordinate with four ligands containing oxygen atoms,[6c,22] so the water number in the metal cation hydration shell (n) is only selected as 2. However, for alkaline-earth metal ions (Mg^{2+}, Ca^{2+}), since the predominant coordination number is 6 for Mg^{2+}, and 7 for Ca^{2+},[23] n values are selected as 4 and 5, respectively. It is well-known that there exists a hydration equilibrium for each hydrated M^{z+} ion, and various hydrates ($M^{z+}(H_2O)_n$, $M^{z+}(H_2O)_{n-1}$, ..., $M^{z+}(H_2O)$) with different water ligands may coexist, although $M^{z+}(H_2O)_n$ is the predominant component. To examine further the effect of the Lewis acidity of metal ions on **FF** PT/ET reactivity, oligohydrates of M^{z+}, which provide models of cations with different binding ability, were also used to bind **FF**. Our calculations also indicated that, in addition to **FF** as a bidentate ligand, only two water molecules can be directly bound to the central Na^+ ion, and other additional water ligands are located at the outer hydration shell. In summary, we mainly explored the coupling effects of a series of hydrated metal ions with $n = 0-2$ for **FF**-$Na^+(H_2O)_n$ and **FF**-$K^+(H_2O)_n$, $n = 1-5$ for **FF**-$Ca^{2+}(H_2O)_n$, and $n = 1-4$ for **FF**-$Mg^{2+}(H_2O)_n$ (Figures S2 and S3). In addition, the effect from the explicit water molecules, which directly bind to the substrate (**FF**), was also examined with and without the participation of metal ions in the outer sphere (Figure S4).

For the following association process, i.e., **FF** + $M^{z+}(H_2O)_n$* → **FF**-$M^{z+}(H_2O)_n$, the binding energy (ΔE_b) can be determined as

$$\Delta E_b = E(\mathbf{FF}) + E(M^{z+}(H_2O)_n^*) - E(\mathbf{FF}\text{-}M^{z+}(H_2O)_n)$$

where E(**FF**-$M^{z+}(H_2O)_n$) and E(**FF**) denote the energies of the corresponding species, **FF**-$M^{z+}(H_2O)_n$ and **FF**, obtained at the B3LYP/6-311++G** level of theory, while $E(M^{z+}(H_2O)_n^*)$ denotes the energy of the hydrated cation ($M^{z+}(H_2O)_n$) with geometry taken from **FF**-$M^{z+}(H_2O)_n$. The counterpoise (CP) method[24] was used to correct basis set superposition error (BSSE) in the calculation of the binding energy.

Natural bond orbital (NBO)[25] analysis was performed to determine the relative significance of individual intermolecular interactions in the context of a donor−acceptor model,[26] and to understand bonding orbitals and electronic properties for all the structures considered here. Natural population analysis, which has been widely applied to many systems and has been recognized to provide physically reasonable results,[26−28] was carried out to get insight into the role of the charge transfer within the complexes.

All calculations reported here were carried out by using the Gaussian 03 suite of programs.[29] The UB3LYP[30] hybrid functional in conjunction with the 6-311++G** basis set[31] was utilized to optimize all geometries fully and to perform the harmonic vibrational analyses for confirming the nature of the corresponding stationary points (minima or transition states). Moreover, the intrinsic reaction coordinate (IRC)[32] analysis was carried out at the same level of theory for all cation-coupled complexes to ensure the connections of the transition states with the desired reactants and products. The restricted molecular orbital contours were used to display the orbital character. The relevant quantities as a function of the cation type and their hydration degrees, and the correlations among several quantities, are displayed in the figures. Other data including Cartesian coordinates, energies and enthalpies, frequencies of all structures, orbital characteristics, and correlations among several quantities are listed in the Supporting Information. In addition, it should be noted that the energies instead of enthalpies are used in the following analyses.

Results and Discussions

PT/ET Exchange Character in FF Mode. As a prelude to a cation modulation mechanism, we first surveyed the PT and ET exchange character between formamide (**F**), the simplest acylamide unit, and its radical (**Fr**) as would be formed by radiation-induced N-dehydrogenation. Geometry optimizations have found that the most favorable mode for **FF** PT/ET is cisoid, with a binding energy of 2.8 kcal/mol with respect to the isolated reactants, **F**+**Fr** (Figure S1 and relevant remarks).[33] It forms an interesting cyclic structure with a C═O···O═C contact $d_{O\cdot\cdot\cdot O}$ = 2.37 Å and a barrier height ΔE_a of 4.3 kcal/mol for the corresponding transition state (**FF**^{ts}).[33] Only the most important geometry parameters are displayed in Figure S1. For **FF**, the spin density (ρ) mainly resides on the two oxygen atoms (0.22 on **F** O_2 and 0.65 on **Fr** O_9), but there is a little on the two nitrogen atoms (0.02 on **F** N_3 and 0.03 on **Fr** N_{10}), which indicates that the dehydrogenation of **F** from the amino group results in an intramolecular ET from the carboxyl oxygen to the amino group radical (•NH−CH═O→NH═CH−O•, a σ-type radical conversion) in the formation of **FF**, before the intermolecular radical exchange reaction (Figure S1). Actually, this intramolecular O→N charge transfer is essential for yielding a net bonding coupling interaction between the two oxygen atoms.[34] For the transition state of **FF** (**FF**^{ts}), molecular orbital analysis shows that the spin density is also mainly located on the two oxygen atoms (0.44/0.44), and its distribution is consistent with the singly occupied molecular orbital (SOMO) (Figures 1, S5). The next highest occupied molecular orbital

(22) (a) Mercuri, F.; Mundy, C. J.; Parrinello, M. *J. Phys. Chem. A* **2001**, *105*, 8423−8427. (b) Buck, U.; Steinbach, C. *J. Phys. Chem. A* **1998**, *102*, 7333−7336.
(23) (a) Jernigan, R.; Raghunathan, G.; Bahar, I. *Curr. Opin. Struct. Biol.* **1994**, *4*, 256−263. (b) Pidcock, E.; Moore, G. R. *J. Biol. Inorg. Chem.* **2001**, *6*, 479−489. (c) Dudev, T.; Lim, C. *J. Am. Chem. Soc.* **2006**, *128*, 1553−1561.
(24) Boys, S. F.; Bernardi, F. *Mol. Phys.* **1970**, *19*, 553−559.
(25) (a) Ditchfield, R. *Mol. Phys.* **1974**, *27*, 789−807. (b) Glendening, E. D.; Badenhoop, J. K.; Reed, A. E.; Carpenter, J. E.; Bohmann, J. A.; Weinhold, F. *NBO*, version 5.0; Theoretical Chemistry Institute, University of Wisconsin: Madison, WI, 2000. (c) Foresman, J. B.; Frisch, A. E.; *Exploring Chemistry With Electronic Structure Methods*, 2nd ed.; Gaussian, Inc.: Pittsburgh, PA, 1996. (d) Clark, T. M.; Grandinetti, P. J. *J. Phys.: Condens. Matter* **2003**, S2387−S2395.
(26) Reed, A. E.; Curtiss, L. A.; Weinhold, F. *Chem. Rev.* **1988**, *88*, 899−926.
(27) Foster, J. P.; Weinhold, F. *J. Am. Chem. Soc.* **1980**, *102*, 7211−7218.
(28) Reed, A. E.; Schleyer, P. v. R. *J. Am. Chem. Soc.* **1990**, *112*, 1434−1445.
(29) Frisch, M. J.; et al. *Gaussian 03*, Revision C.02; Gaussian, Inc.: Wallingford, CT, 2004.
(30) (a) Becke, A. D. *J. Chem. Phys.* **1993**, *98*, 5648−5652. (b) Lee, C.; Yang, W.; Parr, R. G. *Phys. Rev. B* **1988**, *37*, 785−789.
(31) (a) McLean, A. D.; Chandler, G. S. *J. Chem. Phys.* **1980**, *72*, 5639−5648. (b) Krishnan, R.; Binkley, J. S.; Seeger, R.; Pople, J. A. *J. Chem. Phys.* **1980**, *72*, 650−654. (c) Clark, T.; Chandrasekhar, J.; Spitznagel, G. W.; Schleyer, P. v. R. *J. Comput. Chem.* **1983**, *4*, 294−301. (d) Frisch, M. J.; Pople, J. A.; Binkley, J. S. *J. Chem. Phys.* **1984**, *80*, 3265−3269.
(32) (a) Gonzalez, C.; Schlegel, H. B. *J. Phys. Chem.* **1990**, *94*, 5523−5527. (b) Ishida, K.; Morokuma, K.; Kormornicki, A. *J. Chem. Phys.* **1977**, *66*, 2153−2156. (c) Gonzalez, C.; Schlegel, H. B. *J. Chem. Phys.* **1989**, *90*, 2154−2161.

(33) We also estimated the calculational errors for these geometrical parameters and energy quantities by comparing them for **FF**^{ts} at different levels of theory (see Table S4). The deviations among several methods are within 0.05 Å (O···O), 0.01 Å (N···H···N), 0.01 Å (N···H), 0.5° (A_{NHN}) for geometrical parameters, and 1.3 kcal/mol (ΔE_a), 1.5 kcal/mol (ΔE_b), respectively. The deviations of ρ_N and ρ_O are almost equal to zero. Together with the calculated geometrical parameters for **F** (Table S3), all these indicate that B3LYP/6−311++G** can yield the reliable results.
(34) In formamide, both the N and O atoms satisfy the eight-electron rule for bonding. Dehydrogenation at the amino group may generate a stable •NH-CH═O radical, but this radical cannot form the cyclic coupling mode with formamide because the HN-H···•NH single electron H-bond is not as strong as its normal one, and the corresponding ═O···O═ interaction is repulsive. However, the •NH-CH═O radical may be converted into the NH═CH-O• radical by intramolecular O→N electron transfer, favoring the formation of the cyclic coupling mode with formamide, resulting in a normal HN-H···NH two-electron H-bond and a O···O three-electron bond.

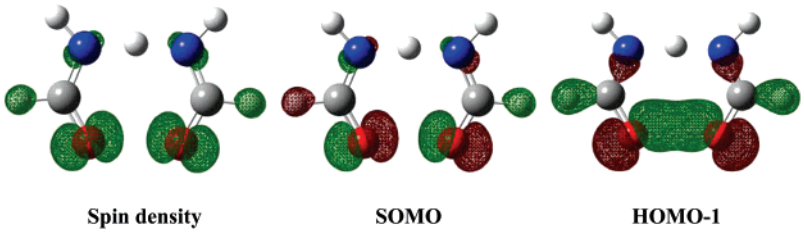

Figure 1. The total spin density (ρ) surface, singly occupied molecular orbital (SOMO), and the next highest doubly occupied molecular orbital (HOMO-1) for **FF**^{ts}. The combination of SOMO and HOMO-1 forms the three-electron σ-bond between two oxygen atoms. See Figure S5 for all the cases studied. The relevant atomic ρ are given in Table S1.

Scheme 2. The Two Proposed PT/ET Mechanisms for Two Distinctly Different Situations: $PCET_s$ (upper) Occurs with Cation-Uncoupled **FF**, or with a Low Electron Affinity Cation-Coupled **FF**, and HAT (lower) Takes Place with a Strong Electron Affinity Group, $M^{z+}(H_2O)_n$, Linking to **FF**[a]

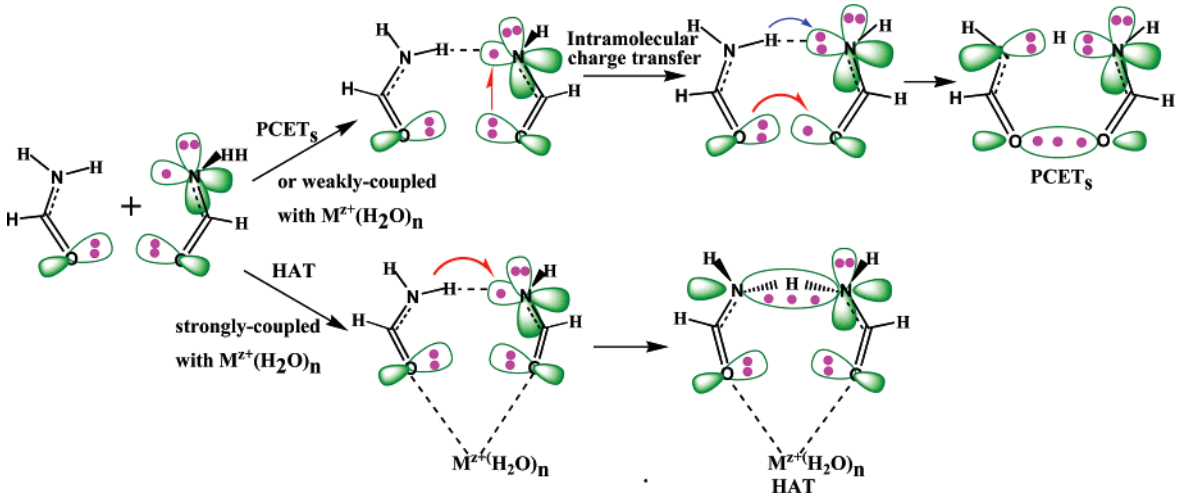

[a] The sp^2-type or p-type orbitals of nitrogen and oxygen are represented by a figure-eight shape, and only the important ones are displayed. All these radicals are σ-type.

(HOMO-1) shows O···O σ-bonding overlap, while the SOMO is a σ*-antibonding orbital between these two atoms. Clearly, the presence of a two-center, three-electron σ-bond between the two oxygen atoms, combined with these two σ-type orbitals, preferentially stabilizes this cyclic transition state structure.[35]

As a result, the proton/electron cooperative exchange reaction in the **FF** cyclic mode occurs via a seven-center cyclic PCET mechanism with PT between the N_3 and N_{10} ($PT_{N\rightarrow N}$) and synchronous ET from the O_2 to O_9 ($ET_{O\rightarrow O}$) (denoted by $PCET_s$), where the subscript s means single-channel ET, as illustrated in the upper pathway in Scheme 2. The two N···H distances at the transition state (1.28 vs 1.04 Å for the free formamide) are short enough to favor PT, while the O···O distance of 2.29 Å reflects the significant overlap of the two oxygens' sp^2 orbitals. Similar to the iminoxyl/oxime case,[11] because of the driving force for yielding net bonding between two oxygen atoms and strengthening the N···HN H-bond, a substantial portion of the electron density is delocalized from the **Fr**'s oxygen to its nitrogen atom, generating the singly occupied oxygen's sp^2 orbital. At the same time, a part of the electron cloud is similarly moved from the **F**'s oxygen to the **Fr**'s oxygen, upon their binding. That is, the electron that will be transferred to **Fr** is already partly localized on **Fr**'s oxygen atom, because of the two-center, three-electron bonding interaction between the two oxygen atoms in the cyclic pretransition state structure. Thus, self-exchange involves PT between the two nitrogen atoms, while cooperatively an electron is transferred in the same direction from the **F** oxygen's sp^2 lone pair to the **Fr** singly occupied oxygen's sp^2 orbital (see the upper Scheme 2).

Cation-Modulated PT/ET Exchange Mechanism. Inspired by the above fact that the formation of the singly occupied oxygen's sp^2 orbital via the charge transfer from **Fr**'s oxygen to its nitrogen favors the cyclic PCET mechanism, we surmised that if the amount of such a charge transfer may be reduced, the O···O bonding coupling interaction should weaken and the corresponding O···O distance should elongate, and thus the proportion of ET from **F** to **Fr** via the O···O channel in the cooperative PT/ET process should decrease. Clearly, the limiting situation should be the cooperative transfer of both electron and proton via the N···N vector as a HAT mechanism.[12−15] Inspection of the structural character of this cyclic **FF** coupling mode reveals that the best way to control the electron density distribution between oxygen and nitrogen atoms should be to bind a Lewis acid to the more negatively charged O···O zone, thus resisting the departure of the electron cloud over the O···O zone. This analysis implies the possibility of modulating the cooperative PCET pathway by changing the relative proportion of electron density distribution between the O···O and the N−H···N zones. To examine this possibility, and in view of the presence of solvated metal ions in biological surroundings, we

(35) At the transition state **FF**^{ts}, the HOMO is a two-electron π*-antibonding orbital, while the HOMO-2 is a two-electron π-bonding orbital. Both distribute over the whole molecular backbone and may be viewed as linear combinations of two local π orbitals located on two molecular fragments, respectively. The net contribution of their combination to the bonding between two molecular fragments is zero.

therefore designed a series of the cation-coupled **FF** PT/ET self-exchange reactions by attaching bioactive hydrated metal ions to the two **FF** oxygen sites (Scheme 1).

(i) Structures. For the reactant complexes bound by the hydrated cations, the **FF** moieties are basically planar and cyclic, with some exceptions that in those bound by the oligohydrated divalent cations the **FF** moieties are almost separated because of the strong binding effect of cations. In contrast, in all the transition state structures, a common structural feature is that the **FF** moieties are planar or near-planar, as in its free mode, and bidentately bind with metal cations via their O···O sites (Figures S2 and S3). An obvious variation for the **FF** moiety upon cation binding, compared with its free state, is the separation of two molecular fragments (**F** and **Fr**). Although the O···O and N···N distances are elongated to different extents in the pre-transition state complexes upon cation binding, slight differences from these distances were observed in the transition states. The O···O distances are also elongated upon cation binding, but the N···N distances are basically unchanged, staying in the narrow range of 2.48−2.55 Å. For example, for the **FF**-$Na^+(H_2O)_n$ $n = 0-2$ series (Figure S2), the O···O distances fall in the range 3.44−3.48 Å, while the N···N distances are 3.31−3.56 Å in the reactant complexes. They are significantly longer than the corresponding ones in **FF** (2.37/2.82 Å). However, for their corresponding transition state structures, $\mathbf{FF}^{ts}$-$Na^+(H_2O)_n$, although the N···N distances (2.55 Å) are almost equal to that (2.54 Å) in $\mathbf{FF}^{ts}$, the O···O distances (2.41−2.47 Å) are considerably elongated by 0.10−0.18 Å compared with that (2.29 Å) in $\mathbf{FF}^{ts}$. Similar changes have also been observed for the **FF**-$K^+(H_2O)_n$ $n = 0-2$ series (Figure S2). For divalent cation-coupled systems, the O···O distances in the reactant complexes are 3.26−3.92 Å for **FF**-$Ca^{2+}(H_2O)_n$ $n = 1-5$, and 3.03−3.47 Å for **FF**-$Mg^{2+}(H_2O)_n$ $n = 1-4$. However, the N···N distances exhibit significant changes subject to the number of water ligands for both series (Figure S3). It should be noted that the N−H···N H-bonds basically disappear for **FF**-Ca^{2+}-$(H_2O)_n$ $n \leq 3$ and for **FF**-$Mg^{2+}(H_2O)_n$ $n \leq 2$, while the corresponding O···O bonding also becomes very weak and even nonexistent. Clearly, this observation may be attributed to the coupling interaction between **FF** and the cation, which is strong enough to break or significantly to weaken the N−H···N H-bond and O···O bonding in this situation. More interesting is that the transition state structures for all the cation-coupled systems considered here involve the same seven-membered cyclic mode with N···N distances of 2.48−2.55 Å (almost equivalent to that of 2.54 Å in the **FF** case). Undoubtedly, such a short distance is a requirement for the most favorable proton/hydrogen transfer. The O···O distances exhibit significant variations depending on the binding ability of the cations. Briefly, the tendency is that the greater the Lewis acidity of the binding cation the more these two bond lengths elongate. Hydration may reduce the Lewis acidity of the metal cations and also their binding ability with **FF** and thus decrease their effect on the structures of the **FF** moieties in the cation-coupled complexes.

Another point that characterizes HAT (mentioned later) should be noted. In the transition state structures coupled with oligohydrated divalent cations, the H_5 atoms are slightly out-of-plane, while in the others the H_5 atoms are in-plane. This phenomenon can be easily interpreted by NBO analysis. When the oligohydrated divalent cations bind to the O···O site, the strong electron-withdrawing force limits the ET from the oxygen sp^2 orbital to the nitrogen singly occupied sp^2 orbital. In this case, to form a strong N···H···N interaction, the in-plane singly occupied sp^2 mixes with the orthogonal-to-plane doubly occupied p-type orbital, generating two new hybrid orbitals for favoring bonding. In the newly formed hybrid orbitals, the p-orbital component in the in-plane one increases, while the s-orbital component in the out-of-plane one increases. The orbital components depend on the binding ability of the metal ions. As a result, the angle between these two newly formed hybrid orbitals enlarges to be more than 90.0°, leading to H_5 departing from the molecular plane. For these oligohydrated Mg^{2+} and Ca^{2+} ions, the corresponding in-plane hybrid orbital in the transition state structure is $sp^{\sim 2.4}$, between sp^2 and sp^3. Both $\tau_{H6N3H5C1}$ and $\tau_{H11N10H5C8}$ dihedral angles are 166.0−167.5°. Actually, this interpretation may apply to all HAT cases considered here.

(ii) Energetics. In both the reactant complexes and transition states, elongation of the O···O distance implies a weakening of the coupling interaction between the two oxygen atoms and, further, a change of the PT/ET cooperative process dynamics. Motivated by these changes, we examined the PT/ET process energetics of these cation-coupled systems. As expected, the calculated barrier heights for the cooperative PT/ET processes in all cation-coupled **FF** systems exhibit significant increases, with the extent of increase dependent on the properties of the bound cations. In detail, for the **FF**-$Na^+(H_2O)_n$ ($n = 0-2$) series, the barrier heights are 13.1, 11.8, and 10.5 kcal/mol for **FF**-Na^+, **FF**-$Na^+(H_2O)$, and **FF**-$Na^+(H_2O)_2$, respectively, all of which are considerably larger than that (4.3 kcal/mol) of the free **FF**. Obviously, the deviation from the free-state barrier height should be mainly attributed to the geometrical changes of **FF** moieties in the reactant complexes relative to their free state because they have more similar transition state geometries. The barrier heights (11.2, 4.4, 4.3 kcal/mol) for **FF**-$K^+(H_2O)_n$ $n = 0, 1, 2$ confirm this analysis. Similarly, since the divalent cations, especially the oligohydrated ones, may cause larger geometry changes of **FF** moieties than the corresponding monovalent cations, the PT/ET barrier heights (25.9−13.4 kcal/mol for **FF**-$Ca^{2+}(H_2O)_n$ $n = 1-5$, 28.1−16.3 kcal/mol for **FF**-$Mg^{2+}(H_2O)_n$ $n = 1-4$) in the divalent-cation-coupled systems are considerably larger than those in the monovalent-cation coupled systems (Table S2).

That the barrier heights increase to different extents for the cation-coupled systems should be attributed to the cation coupling effect. The binding energy is an effective indicator for the binding ability of the hydrated metal ion. The calculated binding energies (ΔE_b) of these hydrated cations with **FF** are in the range of 26.7−174.5 kcal/mol (Table S1). In general, the divalent cations exhibit larger binding energies than the monovalent ones, while, as expected, hydration may reduce the Lewis acidity of cations and thus decrease their binding energies. More interestingly, there is a good correlation between the binding energies and the barrier heights for all the cation-coupled **FF** systems considered here (Figure 2). Intuitively, a large cation effect may result in a large barrier height that is mainly due to two changes: structural deviations of the initial reactants from the free state **FF** and elongation of the O···O distances at the

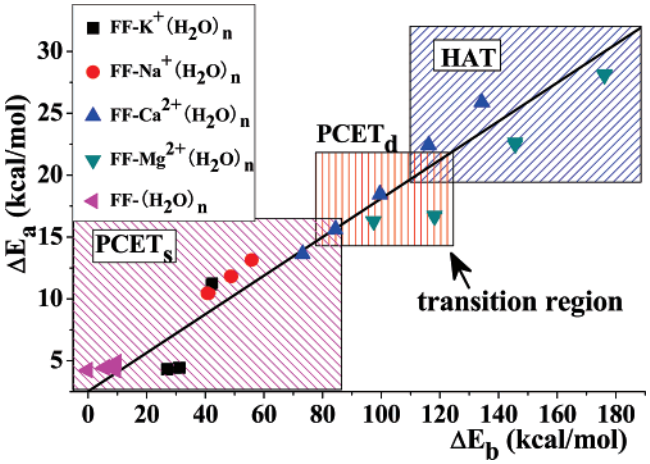

Figure 2. The linear correlation between the binding energies (ΔE_b) and the barrier heights (ΔE_a). Three regions may be recognized for PT/ET, as assisted by different cations and their hydrates. The upper box (blue) is the HAT region, the lower (pink) is the single-ET channel PCET ($PCET_s$) region with $PT_{N\leftrightarrow N}$ and $ET_{O\leftrightarrow O}$, while the middle (orange) is the transition region in which electron transfers occur via two channels at the N↔N and O↔O vectors, respectively ($PCET_d$). For each series of the hydrated cation, the hydration number (n) corresponding to those given in Scheme 1 decreases from left to right.

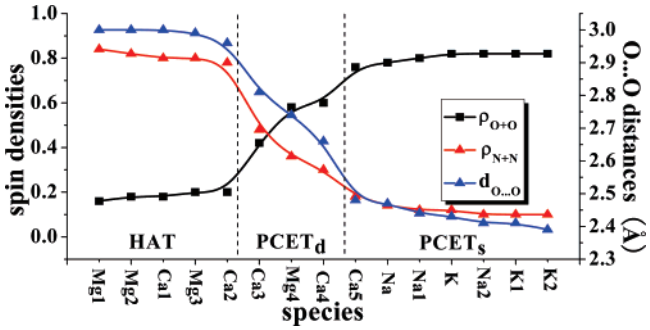

Figure 3. The dependences of the spin densities (ρ_{O+O}, ρ_{N+N}) and the O···O distances (Å) of $\mathbf{FF^{ts}}$-$M^{z+}(H_2O)_n$ on the cation types and their hydration degrees. The symbols **Mn** in the abscissa axis scales denotes $\mathbf{FF^{ts}}$-$M^{z+}(H_2O)_n$.

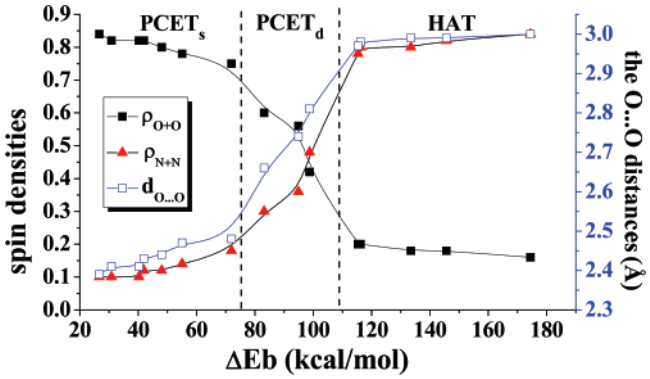

Figure 4. The dependences of the spin densities (ρ_{O+O}, ρ_{N+N}) and the O···O distances (Å) on the binding energies, ΔE_b, for all studied species.

transition states. The dependence of the O···O distances on the binding energies and the cation properties are given in Figures 3 and 4.

(iii) Exchange Mechanism. Intuitively, as mentioned above, association of formamide and its N-dehydrogenated radical as the cyclic coplanar initial reactant, **FF**, requires intramolecular ET from O to N of the N-dehydrogenated **Fr** radical fragment for the purposes of favoring formation of the N···H−N two-electron H-bond and the O···O three-electron bonding. Essentially, this intramolecular ET destabilizes the N-dehydrogenated radical **Fr** moiety satisfying an anti-electronegativity rule; namely, ET from the more electronegative oxygen to the less electronegative nitrogen is thermodynamically nonspontaneous. However, the larger stabilization originating from the formation of the above-noted two bonds relative to the destabilization originating from the intramolecular ET provides the thermodynamic driving force to ensure the existence of **FF**. Therefore, it can be expected that the presence of a Lewis acid around the O···O site may assist the **Fr** O to withdraw a part of the electron cloud back from the N and, as a result, weaken both the N··· HN and O···O bonds and change the cooperative PT/ET pathway.

Inspection of all the calculated data reveals another very interesting aspect. In addition to the above-mentioned barrier height changes induced by the cation coupling, the spin densities (ρ) and SOMOs of the reactants and their transition state complexes in the $\mathbf{FF}$-$M^{z+}(H_2O)_n$ series also present distinct differences, depending on the type and hydration numbers of the cations. In particular, for the transition state complexes coupled by the oligohydrated divalent cations, such as Mg^{2+} and Ca^{2+}, both the ρ and SOMO are mainly localized on the N···H···N vector, causing PT/ET to occur as HAT. However, in the transition state complexes coupled by the monovalent cations, such as Na^+ and K^+, especially for their hydrates, both ρ and SOMO are mainly localized on the O···O vector, making the PT/ET occur as a two-channel PCET ($PCET_s$), with PT via the N···H···N vector ($PT_{N\rightarrow N}$) and ET through the O···O channel ($ET_{O\rightarrow O}$), which is basically similar to the free **FF** case. It is particularly noteworthy that there exists a transition region where the ET channel changes from the N···H···N to the O·· ·O vectors or vice versa. In this region, the transition is gradual, depending on the coupling strength of the cations. An appropriate example to exhibit this variation is the PT/ET exchange process of **FF** coupled by $Ca^{2+}(H_2O)_n$.

For the $\mathbf{FF^{ts}}$-$Ca^{2+}(H_2O)_n$ series, the ρ distribution at the transition state shifts from two nitrogen atoms to two oxygen atoms, as in going from $\mathbf{FF^{ts}}$-$Ca^{2+}(H_2O)$ to $\mathbf{FF^{ts}}$-$Ca^{2+}(H_2O)_5$ (Figures 3 and 5). In $\mathbf{FF^{ts}}$-$Ca^{2+}(H_2O)$, the ρ is mainly localized on two nitrogen atoms (0.40/0.40) along the N···H···N vector. When the water ligand number increases, a single electron is transferred from two oxygen atoms to two nitrogen atoms. In the $\mathbf{FF^{ts}}$-$Ca^{2+}(H_2O)_3$ case, the spin densities over the two nitrogen atoms (0.24/0.24) are nearly equal to those over the two oxygen atoms (0.21/0.21), while a further increase to $\mathbf{FF^{ts}}$-$Ca^{2+}(H_2O)_5$ leads to ρ located mainly on the two oxygen atoms (0.38/0.37) with only a little on the two nitrogen atoms (0.09/0.09).

Similar tendencies are also observed from monitoring the orbital character (Figures 5, S7). In $\mathbf{FF^{ts}}$-$Ca^{2+}(H_2O)$, the SOMO largely localizes on the two NH groups, with small coefficients on the two oxygen sites. On the other hand, the O···O distance at this transition state is 2.99 Å, which is too long to be favorable to ET between the oxygen pair. Clearly, this is a HAT mechanism.[12−15] Similarly, $\mathbf{FF^{ts}}$-$Ca^{2+}(H_2O)_2$ also obeys the HAT mechanism.

In $\mathbf{FF^{ts}}$-$Ca^{2+}(H_2O)_3$, although the SOMO is antibonding and the third highest occupied molecular orbital (HOMO-2) is bonding, both delocalize over the whole molecular plane. Their

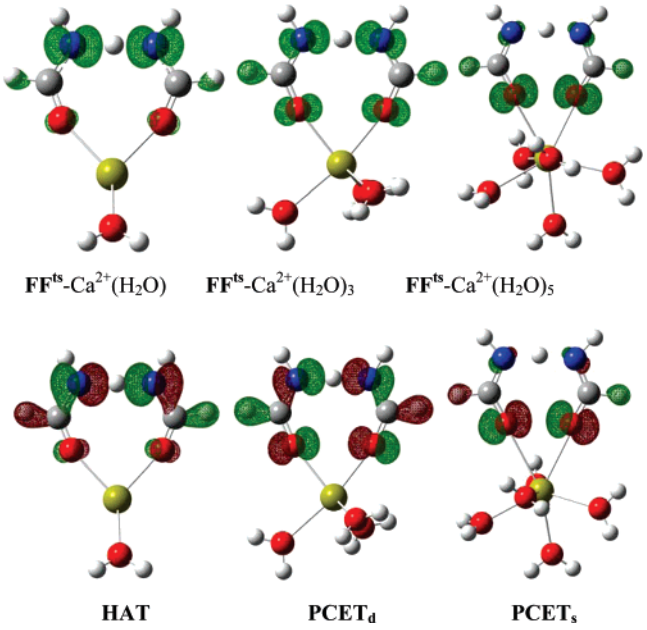

Figure 5. The total spin density surfaces (upper), the singly occupied molecular orbitals (lower), and the corresponding PT/ET types for **FF**^{ts}-$Ca^{2+}(H_2O)$, **FF**^{ts}-$Ca^{2+}(H_2O)_3$, and **FF**^{ts}-$Ca^{2+}(H_2O)_5$.

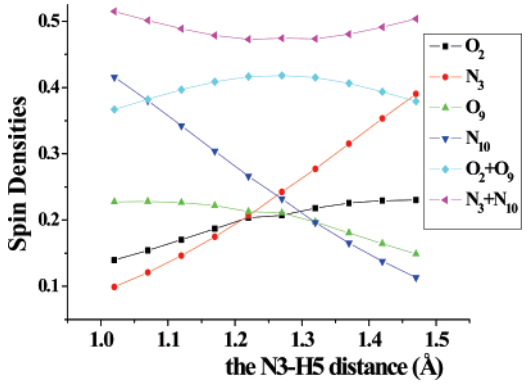

Figure 6. The variations in spin densities on the O_2, N_3, O_9, and N_{10} atoms with H_5 migration from the N_3 to N_{10} in the **FF**^{ts}-$Ca^{2+}(H_2O)_3$ case. More importantly, the sum of the two O atoms (two N atoms) changes in a narrow range (the highest two curves).

combination contributes to a three-electron weak σ-bond, which describes the interaction between the **F** and **Fr** moieties in **FF**^{ts}-$Ca^{2+}(H_2O)_3$. More importantly, this interaction allows the shifting of a proton from **F**$-NH_2$ to **Fr**$-NH^{\bullet}$ and the transfer of an electron from **F** to **Fr** via two channels: N→N and O→O. The ρ changes caused by H_5 migration from NH_2 to $NH^{\bullet}$ in this case also verify the above analysis by the fact that the total ρ_N varies in a narrow range of 0.47−0.51 and the total ρ_O is also basically unchanged (0.37−0.42) (Figure 6). Overall, when $Ca^{2+}(H_2O)_3$ links to two oxygen atoms of **FF**, PT/ET occurs via a seven-center, cyclic PCET mechanism with the shifting of a proton from NH_2 to $NH^{\bullet}$ and the transfer of an electron from **F** to **Fr** through two in-plane channels: N→N and O→O (noted as $PCET_d$, where the subscript d means the double-channel ET).

However, in **FF**^{ts}-$Ca^{2+}(H_2O)_5$, the in-plane SOMO and HOMO-1 almost entirely localize in the O···O vicinity despite the different bonding characteristics (Figure 7). As a result, their combination contributes to a two-center three-electron O···O bond, which allows the transfer of an electron from one oxygen

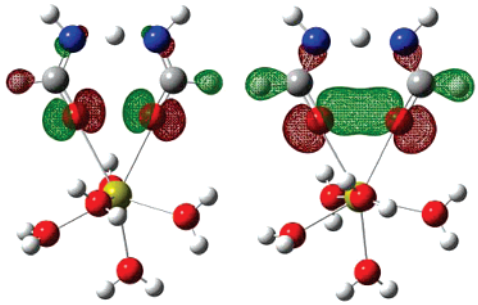

Figure 7. The singly occupied molecular orbital (SOMO, left) and a doubly occupied molecular orbital (HOMO-1, right) mainly reside on the two oxygen atoms, with small coefficients on the two nitrogen atoms, for **FF**^{ts}-$Ca^{2+}(H_2O)_5$. Their combination forms the O···O three-electron bond.

to another, viz., the single-channel ET. Also, the O···O distance in **FF**^{ts}-$Ca^{2+}(H_2O)_5$ is only 2.48 Å, short enough to be favorable to ET. Thus, it can be concluded that in this case the PT/ET in the **FF** moiety takes place via a seven-center, cyclic PCET mechanism with $PT_{N\rightarrow N}$ and $ET_{O\rightarrow O}$ (as denoted as $PCET_s$).

Similar analyses can be made for the cases catalyzed with other hydrated metal ions. In general, PT/ET in the **FF**-$Na^+(H_2O)_n$ and **FF**-$K^+(H_2O)_n$ cases (Figures S8 and S9) are like those in **FF**-$Ca^{2+}(H_2O)_5$, following $PCET_s$, while PT/ET in **FF**-$Mg^{2+}(H_2O)_n$ (Figure S10) adopts HAT for $n = 1-3$ (similar to **FF**-$Ca^{2+}(H_2O)_{1-2}$) or $PCET_d$ for $n = 4$ (similar to **FF**-$Ca^{2+}(H_2O)_{3-4}$). The overall tendencies are that the high valent cation couplings may promote HAT and the low valent cation couplings favor $PCET_s$, and that cation hydration may increase the preference for $PCET_s$. The spin density diagram displayed in Figure 3 provides a clear rationale for this classification.

In view of the possible coupling interaction of the Lewis acid/base with **FF**, we examined the effect of water molecules without metal ion participation (Figure S4). Two situations were considered: direct H-bonding of H_2O in a water cluster $(H_2O)_{1-8}$ to the oxygen sites and direct interaction of the oxygens of water molecules with the N−H sites. The binding energies of these water oligomer clusters are 5.3−17.7 kcal/mol, significantly smaller than those (26.7−174.5 kcal/mol) of hydrated cations. As a result, the geometrical deformations of **FF** and **FF**^{ts} moieties are very small compared with their free states (the N···N/O···O distances: 2.82∼2.85/2.38∼2.45 vs 2.82/2.37 Å), and the corresponding barrier heights range from 4.3 to 4.8 kcal/mol, also very close to that (4.3 kcal/mol) in the free state. These observations indicate that water solvation cannot change the $PCET_s$ mechanism of **FF** moieties.

In addition, as an example, the effect of the indirect coupling of $Ca^{2+}(H_2O)_6$ to the two oxygen atoms via water (the ligand) bridge was also examined. Although its effect is slightly larger than the direct hydration, the catalysis in such a mode is considerably smaller than the direct metal ion binding. Furthermore, **FF** has greater nucleophilicity than a water molecule, and the replacement of two inner-shell water ligands of $M^{2+}(H_2O)_n$ by **FF** is exothermic and thermodynamically allowed.[36] Therefore, the inner shell binding of **FF** with $M^{z+}(H_2O)_n$ by removing two inner-shell water ligands is predominant.

Clearly, the above observations may be attributed to charge migrations, structural changes, and electronic interactions.

(36) We examined the thermodynamics associating with the ligand exchange process: $M^{z+}(H_2O)_n$ + **FF** = **FF**-$M^{z+}(H_2O)_{n-2}$ + $2H_2O$. The energy changes for three selected hydrated metal ions are exothermic: −18.0 ($Ca^{2+}(H_2O)_6$), −2.1 ($Ca^{2+}(H_2O)_7$, and −18.5 ($Mg^{2+}(H_2O)_6$) kcal/mol, respectively.

Compared with the cation-uncoupled **FF** discussed above, the hydrated metal ion coupling may effectively inhibit its PT/ET dynamics and change the ET channel, revealing the possibility of metal cations and their hydrates in regulating this kind of radical exchange reactions.

As mentioned above, there is a good correlation between the PT/ET barrier heights, ΔE_a, and the binding energies, ΔE_b, of hydrated cations with **FF** (Figure 2). More interesting is that this correlation line may be approximately divided into three regions: HAT, $PCET_d$, and $PCET_s$, as marked in Figure 2. Various hydrated metal ions may fall in the given regions where they function as discussed for PT/ET. This correlation may represent a general phenomenon and could be used to interpret the role of all possible hydrated metal ions in regulating the mechanism of **FF** PT/ET.

Similarly, there also exists a correlation between ΔE_b and the O···O contact distance. The spin density distributions also exhibit an intriguing dependence on the binding energies, ΔE_b, of cations, which leads to a classification and linkage of the three PT/ET mechanisms of HAT, $PCET_d$, and $PCET_s$ (Figure 4). Together with the $\Delta E_a - \Delta E_b$ correlation and hydration effect, they imply that the nature of the modulation should be due to the N→O electron-return-induced weakening of the special O•••O interaction induced by the coupling to hydrated metal ions. The main tendency is that the strong binding ability of a hydrated cation favors the HAT mechanism, and inversely, a weak binding ability favors the PCET mechanism. Thus, the binding ability of the hydrated metal ions is the essential feature that regulates the **FF** PT/ET pathway.

It should be noted that the role of the hydrated cations in regulating the ET channel is as a side-modulator instead of as an intercalator.

Concluding Remarks

In summary, hydrated metal ions can regulate the **FF** PT/ET cooperative mechanism, spanning a single-pathway HAT, or a variable-pathway PCET by changing the ET channel. The regulation essentially originates from the changes in the O···O bond strength in the transition state, subject to the binding ability of hydrated metal ions. In general, the high valent metal ions and those with large ΔE_b can promote HAT, and the low valent metal ions and those with small ΔE_b favor PCET. Additionally, hydration may reduce the Lewis acidity of the cations, thus favoring PCET, and moving PCET from $PCET_d$ to $PCET_s$. Furthermore, significant increases of the PT/ET barrier heights due to the metal cation couplings imply a reduction in the rate of a PT/ET process. Thus, metal cation coupling can modulate not only the PT/ET pathway but also its rate. In addition, although our conclusions are drawn from the effect of the alkali metal ion and alkaline earth metal ion hydrates, they may represent a general regularity and can be safely applied to interpret the modulation role of any metal ion complexes. For this **FF** system, two distinctly different cases are HAT (corresponding to the larger cation coupling effect) and $PCET_s$ (corresponding to the smaller one, even zero), respectively. It can be expected that the PT/ET pathways modulated by any metal ion complex can fall in the range of $HAT-PCET_s$.[37]

The finding that a microscopic ET mechanism in acylamide units exists, in which the electron migration channel is governed by varying the hydrated metal ion properties, may provide additional insights into the cooperative PT/ET mechanism. Understanding the basic principles for the modulation of the PT/ET mechanism and rate may aid in the design of molecular switches via changing the conductance of a molecular unit in nanoelectronic devices. It also presents the impetus for further experimental tests of the PT/ET mechanism modulated by metal ion complexes and motivates continued theoretical explorations.

Acknowledgment. We sincerely thank the referees for their extremely helpful comments and also thank Prof. R. I. Cukier and Dr. Y. Wang for improving the presentation of the work. This work is supported by NSFC (20633060, 20573063), NCET, sdNSF(Z2003B01), and the Virt Lab for Comput Chem of CNIC-CAS. Calculations were performed on the HPCC at SDU and SCC of CNIC-CAS.

Supporting Information Available: The complete citation for reference 29 as well as the calculated molecular geometries, spin densities, orbital characters, relevant energetics, and Cartesian coordinates for all reactants and the transition state complexes and correlations among several quantities. This material is available free of charge via the Internet at http://pubs.acs.org.

JA071194M

(37) Although the oligohydrates of the metal ions are not predominant species, we can use them to model the hydrated metal ions with large binding energies or Lewis acidity. The binding of these kinds of cations with **FF** favor HAT. To verify this conclusion, we also examined the effect of a trivalent cation Sc^{3+} hydrate, **FF**-$Sc^{3+}(H_2O)_4$ (**FF**+$Sc^{3+}(H_2O)_6$→**FF**-Sc^{3+}-$(H_2O)_4$+$2H_2O$) on the **FF** PT/ET mechanism. Results (at the transition state, $\rho_{N3+N10} = 0.88$, $\rho_{O2+O9} = 0.12$) indicate that **FF**-$Sc^{3+}(H_2O)_4$ obeys the HAT mechanism.